

Cotangent states of the electromagnetic field: Squeezing and phase properties

Pierre Meystre,* John Slosser, and Martin Wilkens

Optical Sciences Center, University of Arizona, Tucson, Arizona 85721

(Received 26 December 1990)

We analyze the phase and squeezing properties of the cotangent states of the electromagnetic field. We calculate the phase distribution, phase variance, and number-phase uncertainty product for these states. Under appropriate conditions, the phase distribution develops oscillations resulting from the formation of states, reminiscent of macroscopic superpositions. In other cases the cotangent states are nearly minimum number-phase uncertainty states, emulating the coherent states. We also study the quadrature squeezing properties of the cotangent states and find that under a wide range of conditions they are highly squeezed.

I. INTRODUCTION

In a recent series of publications,^{1,2} we introduced a new class of states of the electromagnetic field, the so-called tangent and cotangent states. These states can be prepared in a single-mode, lossless cavity pumped by a stream of polarized two-level atoms. Under appropriate conditions, these states resemble macroscopic superpositions or alternatively may exhibit sub-Poissonian photon statistics. In further studies, we found that these nonclassical properties are surprisingly robust under the effects of cavity damping.³ The present paper extends this earlier work by calculating the phase and squeezing properties of the cotangent states.

The problems associated with developing a single Hermitian phase operator for the harmonic oscillator are well known as is the troublesome interpretation of the phase-number commutator.⁴⁻⁷ Recently, Pegg and Barnett have used a semiclassical approach to circumvent these problems.⁸⁻¹⁰ This approach leads to a well-defined Hermitian phase operator and a phase-number uncertainty product which takes into account the periodicity of the phase variable. In this paper we use this formalism to calculate the phase properties of interest.

The squeezing of a single-mode coherent field interacting with a single two-level atom has been studied,^{11,12} with results indicating that transient squeezing can approach 100% as the field intensity increases.¹² Here we calculate the squeezing of the cotangent states and find a somewhat analogous result.

The paper is organized as follows. Section II reviews the circumstances under which tangent and cotangent states can be generated in a lossless micromaser. We give the photon statistics and basic properties of these states. Section III analyzes the phase properties of the cotangent states. We compute the phase distribution, phase variance, and number-phase uncertainty product. These results indicate that for a large range of parameter values the cotangent states are nearly minimum uncertainty number-phase states, while under other circumstances the phase distribution develops oscillations. In Sec. IV we evaluate the quadrature squeezing of the cotangent

states. We find that the cotangent states may be highly squeezed. Finally, Sec. V is a summary and conclusion.

II. REVIEW OF THE COTANGENT STATES

The conditions under which the intracavity field of a lossless, single-mode cavity pumped by a sequence of polarized two-level atoms can evolve to tangent and cotangent states include (a) the fact that the field frequency must be resonant with the atomic transition frequency ω , and (b) the existence of trapping states of the field.¹³ These trapping states are number states $|M\rangle$ satisfying

$$\kappa\sqrt{M+1}\tau=q\pi \tag{2.1}$$

(where q is an integer), i.e., they are such that the Bloch vector of an initially excited two-level atom interacting with the field in the state $|M\rangle$ undergoes a $2q\pi$ rotation during the interaction time τ . Similarly, an atom initially in its ground state undergoes a $2q\pi$ rotation for $\kappa\sqrt{N}\tau=q\pi$, a condition sometimes referred to as a down-trapping condition. If the field density matrix is initially confined between two trapping states $|N\rangle$ and $|M\rangle$ with $M > N$, $\kappa\sqrt{N}\tau=q\pi$, and $\kappa\sqrt{M+1}\tau=p\pi$ such that q is even and p is odd, then the steady state reached by the field is^{1,2}

$$|\text{cot}\rangle = \sum_{n=N}^M s_n |n\rangle, \tag{2.2}$$

where

$$s_n = C(-i)^n(\alpha/\beta)^n \prod_{j=1}^n \cot(\kappa\tau\sqrt{j}/2). \tag{2.3}$$

(The minus sign in these probability amplitudes differs from the convention of Refs. 1 and 2 and follows the notations of Ref. 14.) Here C is a normalization constant and the polarized atoms are injected inside the cavity in the state

$$|\psi_{\text{at}}\rangle = \alpha|a\rangle + \beta|b\rangle, \tag{2.4}$$

where α and β are the upper and lower atomic-state probability amplitudes, and τ is the interaction time of each atom with the field mode.

Similarly, if q is odd and p even, the field evolves to the pure state

$$|\tan\rangle = \sum_{n=N}^M t_n |n\rangle, \quad (2.5)$$

with

$$t_n = C'(i)^n (\alpha/\beta)^n \prod_{j=1}^n \tan(\kappa\tau\sqrt{j}/2). \quad (2.6)$$

In practice, the field initial conditions usually include a finite probability of occupation of the vacuum state, so that cotangent states with $N=0$ are of particular relevance. We concentrate on this special case throughout the remainder of this paper. For notational convenience, we also designate cotangent states bound between the vacuum and a trapping state such that an initially excited atom undergoes a $2p\pi$ rotation as p -cotangent states. Reference 1 shows that the photon statistics of the 1-cotangent states are sub-Poissonian for all M and for all probability amplitudes α . The photon statistics of the 3-cotangent states are also sub-Poissonian, except in the approximate range $0.2 \leq |\alpha|^2 \leq 0.4$, where they are bimodal with a peak at $n=0$ and the other one near $n=0.6M$. In this region, the cotangent states acquire characteristics reminiscent of macroscopic superpositions.^{1,2} For higher values of p , multi-peaked photon statistics are possible, the maximum number of peaks being given by $(p+1)/2$.

III. PHASE PROPERTIES

Consider an infinite set of so-called phase states^{5,15}

$$|\theta\rangle = (2\pi)^{-1/2} \sum_{n=0}^{\infty} \exp(in\theta) |n\rangle, \quad (3.1)$$

which evolve in time according to

$$\exp(-i\omega a^\dagger at) |\theta\rangle = |\theta - \omega t\rangle. \quad (3.2)$$

Despite this desirable property, these phase states are plagued by a number of difficulties, the most important being that they are not normalizable. Furthermore, they are not orthogonal, $\langle \theta' | \theta \rangle \neq \delta(\theta' - \theta)$, and are not the eigenfunctions of any Hermitian operator.

To circumvent this problem, Pegg and Barnett⁸⁻¹⁰ recently introduced the finite set of states

$$|\theta_m\rangle = (l+1)^{-1/2} \sum_{n=0}^l \exp(in\theta_m) |n\rangle, \quad m=0, 1, \dots, l \quad (3.3)$$

where the $l+1$ values of θ_m are given by

$$\theta_m = \theta_0 + \frac{2\pi}{l+1} m. \quad (3.4)$$

For a given value of θ_0 these states form a complete orthonormal basis set on the $(l+1)$ -dimensional Hilbert space. Taking for concreteness $\theta_0=0$, a Hermitian operator $\hat{\phi}_l$ can now be defined as

$$\hat{\phi}_l \equiv \sum_{m=0}^l \theta_m |\theta_m\rangle \langle \theta_m|, \quad (3.5)$$

where this operator is single valued on the interval $\theta_m \in [0, 2\pi[$. The operator $\hat{\phi}_l$ has $l+1$ eigenvalues and can be interpreted as a phase operator only as l tends to infinity. Pegg and Barnett's prescription is to evaluate any observable of interest on the finite basis (3.3) and then take the limit $l \rightarrow \infty$.

Applying this recipe to the problem at hand, we note that the probability that the cotangent state $|\cot\rangle$ is in the state $|\theta_m\rangle$ is given by

$$P_{\theta_m} \equiv |\langle \cot | \theta_m \rangle|^2 = \frac{1}{l+1} \sum_{n,n'=0}^M s_n s_{n'}^* e^{i(n-n')\theta_m}, \quad (3.6)$$

and quantum-mechanical expectation values of powers of the Pegg-Barnett operator $\hat{\phi}_l$ are given by

$$\langle \hat{\phi}_l^v \rangle = \sum_{m=0}^l \theta_m^v P_{\theta_m}. \quad (3.7)$$

Numerically, such expectation values are evaluated by taking $l \gg M$. The convergence of the result is then tested by checking the independence of the results on larger values of l . For future use, we finally note that in the limit $l \rightarrow \infty$, the discrete set of probabilities (3.6) is replaced by the probability density $P(\theta)$,

$$P(\theta) = \frac{1}{2\pi} \sum_{n,n'=0}^M s_n s_{n'}^* e^{i(n-n')\theta}, \quad (3.8)$$

and $\lim_{l \rightarrow \infty} \langle \hat{\phi}_l^v \rangle$ is abbreviated as $\langle \hat{\phi}^v \rangle$.

Figures 1(a) and 1(b) display the probabilities P_{θ_m} as a function of the upper-state population $|\alpha|^2$ of the injected atoms for 1- and 3-cotangent states, respectively. Here we have taken $l=10000$, and the discrete probabilities have been connected by a line. For such a high truncation value, these probabilities are practically indistinguishable from the continuous distribution function $P(\theta)$. In both figures the cotangent states are bound between the vacuum $|0\rangle$ and the trapping state $|20\rangle$. Three different regimes can be distinguished. For very weakly excited atoms, $|\alpha|^2 \ll 1$, both the 1- and 3-cotangent states resemble the vacuum state. Here the phase of the field is completely undetermined and $P(\theta) \cong 1/2\pi$. As $|\alpha|^2$ is increased, the mean number of photons of the 1-cotangent state increases monotonically, as does its sub-Poissonian character.^{1,2} There is, however, a large range of upper-state populations where it resembles a coherent state. In this region the phase distribution $P(\theta)$ develops a well-defined maximum, indicating that the phase of the field becomes reasonably well defined. As the injected atoms become more and more inverted, however, this character disappears: For $|\alpha|^2 \rightarrow 1$, the cotangent state degenerates into the number state $|M\rangle$, in which limit $P(\theta)$ becomes again constant.

Although the 3-cotangent states behave in the same qualitative way in the limits $|\alpha|^2 \rightarrow 0$ and 1, the domain of intermediate inversions is completely different. After a region of small $|\alpha|^2$, where $P(\theta)$ is essentially constant, we observe the appearance of oscillations in $P(\theta)$. The

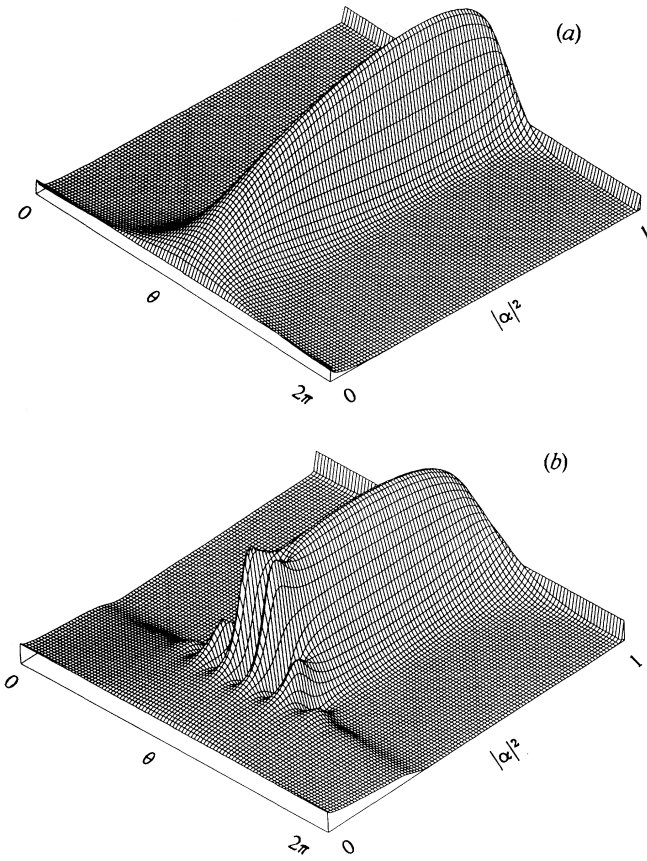


FIG. 1. Phase distribution $P(\theta)$ vs $|\alpha|^2$ for the (a) 1-cotangent states and (b) 3-cotangent states bound between the vacuum state $|0\rangle$ and the trapping state $|20\rangle$.

onset of these oscillations corresponds precisely to the onset of “macroscopic superpositions” characterized by bimodal photon statistics.

These oscillations can be understood intuitively by mimicking the cotangent states by the simple superposition

$$|\text{cot}\rangle \cong c_0|0\rangle + c_m|m\rangle, \quad (3.9)$$

where $m \cong M$. In this case we have

$$P(\theta)d\theta \cong \frac{1}{2\pi} \{ |c_0|^2 + |c_m|^2 + 2|c_0c_m| \cos[m(\theta + \psi)] \} d\theta, \quad (3.10)$$

where $c_0c_m^* = |c_0c_m| \exp(i\psi)$. This simple argument shows that the oscillations in the phase distribution can be interpreted as resulting from the interferences in Fock space¹⁶ between the two “macroscopically” separated quantum states of the superposition. Of course, the situation is somewhat more complicated for cotangent states, as they cannot be described precisely as the sum of only two number states. These oscillations therefore have the same origin as the oscillations in the Q function discussed previously.¹⁷ In the case of 1-cotangent states, the pho-

ton statistics always remain single peaked, and the quantum interferences in $P(\theta)$ are washed out.

Figure 2 shows the standard deviation of the phase $\sigma_\theta = (\langle \phi^2 - \langle \phi \rangle^2)^{1/2}$ versus $|\alpha|^2$ for 1-cotangent states (dashed line) and 3-cotangent states (solid line) bound between the vacuum $|0\rangle$ and the trapping state $|20\rangle$. In the limits $|\alpha|^2 \rightarrow 0$ and 1, the cotangent states reduce to the number states $|0\rangle$ and $|20\rangle$, respectively, and have a completely random phase distribution with variance $\pi^2/3$. The standard deviation of the phase of the 1-cotangent states decreases with increasing $|\alpha|^2$ until $|\alpha|^2 \cong 0.90$, at which point the field begins to take on the characteristics of the upper trapping state $|20\rangle$ and the phase variance returns to $\pi^2/3$. Notice that the standard deviation in phase of the 3-cotangent states is somewhat larger than that for the 1-cotangent states. It also drops off significantly at $|\alpha|^2 \cong 0.36$, a signature of the transition of the 3-cotangent states photon statistics from a bimodal to a single-peaked distribution corresponding to a state of relatively well-defined phase.

In the above graphs, we have chosen the relative phase between the atomic probability amplitudes α and β such that $\langle \hat{\phi} \rangle = \pi$, i.e., the expectation value of the phase is at the center of the phase window $[0, 2\pi]$ and the standard deviation is minimized. Clearly, cotangent states with the same photon statistics but with different mean phases than the case shown here would have different phase variances. This result, due to the arbitrariness in the choice of the 2π interval over which the phase is measured, has been discussed by Pegg and Barnett.⁹

In Figs. 3(a) and 3(b) we show the uncertainty product $\Delta n \Delta \phi$ (solid lines) versus $|\alpha|^2$ for 1- and 3-cotangent states bound between the vacuum $|0\rangle$ and upper trapping state $|20\rangle$. Pegg and Barnett⁹ as well as Shapiro, Shepard, and Wong¹⁸ have shown, using the phase operator (3.5), that the uncertainty relation between number and phase is given by

$$\Delta n \Delta \phi \geq \frac{1}{2} [1 - 2\pi P(\theta_0)]. \quad (3.11)$$

Only when $P(\theta_0)$ is zero do we recover the “convention-

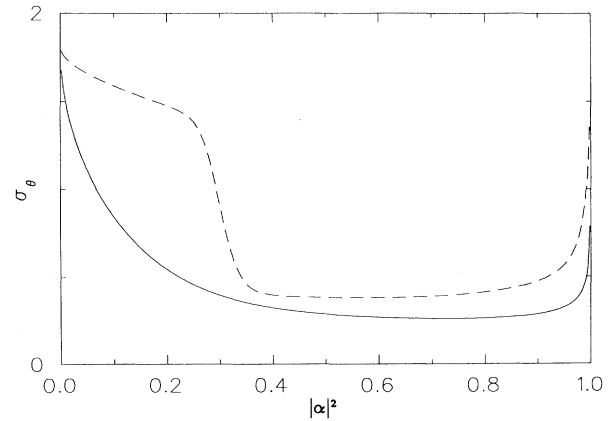


FIG. 2. Standard deviation in phase σ_θ vs $|\alpha|^2$ for the 1-cotangent states (solid line) and 3-cotangent states (dashed line) bound between the vacuum $|0\rangle$ and the trapping state $|20\rangle$.

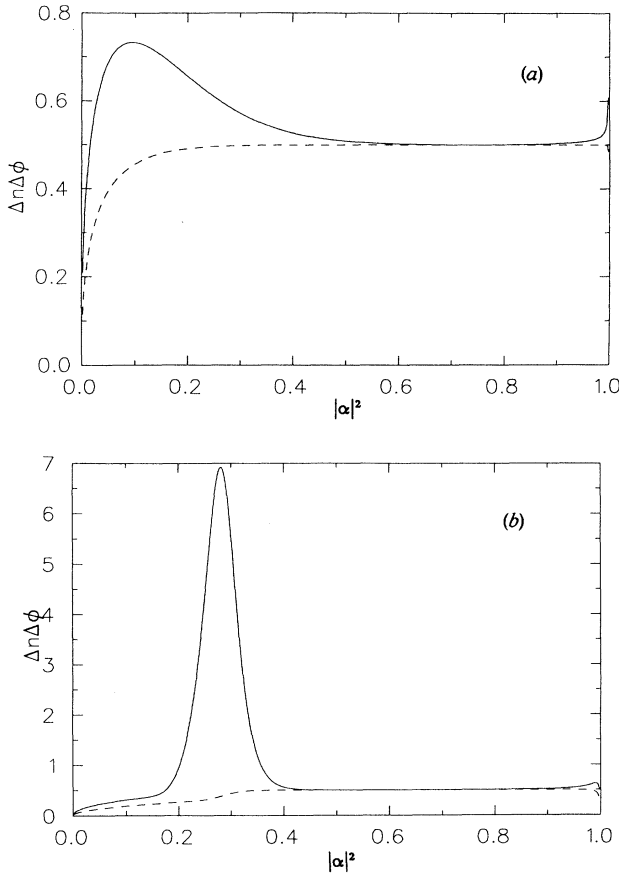


FIG. 3. (a) Uncertainty product $\Delta n \Delta \phi$ (solid line) vs $|\alpha|^2$ for the 1-cotangent states bound between the vacuum $|0\rangle$ and trapping state $|20\rangle$. The dashed line shows the minimum value $\frac{1}{2}[1 - 2\pi P(\theta_0)]$, where $\theta_0 = 0$. (b) Same for the case of the 3-cotangent states.

al" uncertainty principle; otherwise, $P(\theta_0)$ enables the number-phase uncertainty product of some states to fall below $\frac{1}{2}$. For example, any number state has a constant $P(\theta_0)$ equal to $1/2\pi$, resulting in an uncertainty product of zero. This is because for such states $\Delta n = 0$ and $\Delta \phi$ is always finite. The dashed lines of Fig. 3 are the right-hand side of Eq. (3.11). We see in both Figs. 3(a) and 3(b) that at intermediate values of $|\alpha|^2$, $\Delta n \Delta \phi$ is much larger than the minimum allowed uncertainty, but as $|\alpha|^2$ increases past 0.70, the product decreases to about its minimum value. Finally, as $|\alpha|^2$ approaches 1, the cotangent states degenerate into the number state $|20\rangle$, where $\Delta n \Delta \phi$ and $\frac{1}{2}[1 - 2\pi P(\theta_0)]$ return to zero.

IV. SQUEEZING PROPERTIES

In this section, we investigate the quadrature squeezing properties of the 1- and 3-cotangent states. Introducing the quadrature operators a_1 and a_2 via

$$a = a_1 + ia_2, \quad (4.1)$$

we have the uncertainty relation

$$\Delta a_1 \Delta a_2 \geq \frac{1}{4}. \quad (4.2)$$

Squeezing is said to occur if the fluctuations in one of the quadratures a_1 or a_2 satisfy the relation

$$(\Delta a_i)^2 < \frac{1}{4}, \quad i = 1, 2. \quad (4.3)$$

In terms of a and a^\dagger , the variances of a_1 and a_2 are

$$\begin{aligned} (\Delta a_1)^2 &= \langle (a_1 - \langle a_1 \rangle)^2 \rangle \\ &= \frac{1}{4}(4\langle a^\dagger a \rangle + 1 + \langle a^2 \rangle + \langle a^{\dagger 2} \rangle - \langle a + a^\dagger \rangle^2) \end{aligned} \quad (4.4a)$$

and

$$\begin{aligned} (\Delta a_2)^2 &= \langle (a_2 - \langle a_2 \rangle)^2 \rangle \\ &= \frac{1}{4}(4\langle a^\dagger a \rangle + 1 - \langle a^2 \rangle - \langle a^{\dagger 2} \rangle + \langle a - a^\dagger \rangle^2). \end{aligned} \quad (4.4b)$$

For the cotangent state (2.2), this gives

$$\begin{aligned} (\Delta a_1)^2 &= \frac{1}{4} \sum_{n=0}^M (4n|s_n|^2 + 1 + \sqrt{n(n-1)}s_{n-2}^*s_n \\ &\quad + \sqrt{(n+2)(n+1)}s_{n+2}^*s_n) \\ &\quad - \left[\sum_{n=0}^M (\sqrt{n}s_{n-1}^*s_n + \sqrt{n+1}s_{n+1}^*s_n) \right]^2 \end{aligned} \quad (4.5a)$$

and

$$\begin{aligned} (\Delta a_2)^2 &= \frac{1}{4} \sum_{n=0}^M (4n|s_n|^2 + 1 - \sqrt{n(n-1)}s_{n-2}^*s_n \\ &\quad - \sqrt{(n+2)(n+1)}s_{n+2}^*s_n) \\ &\quad + \left[\sum_{n=0}^M (\sqrt{n}s_{n-1}^*s_n - \sqrt{n+1}s_{n+1}^*s_n) \right]^2. \end{aligned} \quad (4.5b)$$

In Fig. 4 we show the squeezing of the cotangent states. The variances $(\Delta a_1)^2$ (solid line), $(\Delta a_2)^2$ (dashed line), and the product $(\Delta a_1)(\Delta a_2)$ (dotted line) are plotted versus $|\alpha|^2$ for the 1- and 3-cotangent states in Figs. 4(a) and 4(b), respectively. Here the relative phase between the probability amplitudes α and β is set at $\pi/2$. The maximum squeezing in quadrature a_1 for the 1-cotangent states is approximately 67%, while it reaches about 41% in the 3-cotangent states. Figure 4(a) shows that when $|\alpha|^2 \leq 0.9$, the uncertainty product $(\Delta a_1)(\Delta a_2)$ is only slightly larger than $\frac{1}{4}$. The peak in the variances in the range $0.25 \leq |\alpha|^2 \leq 0.36$ of Fig. 4(b) corresponds to the region where the cotangent states exhibit bimodal photon statistics. These results are consistent with those of Qamar, Zaheer, and Zubairy,¹⁹ who computed the evolution of squeezing as the field evolved to a 1-cotangent state in steady state. For the case of $M = 20$ and $|\alpha|^2 = 0.7$, they found the 1-cotangent state to have variances $(\Delta a_1)^2 \approx 0.1$, $(\Delta a_2)^2 \approx 0.5$.

Figure 5 shows the standard deviations Δa_1 (solid line) and Δa_2 (dashed line), as well as the uncertainty product $(\Delta a_1)(\Delta a_2)$ (dotted line) versus the relative phase ϕ between the probability amplitudes α and β . Here we have

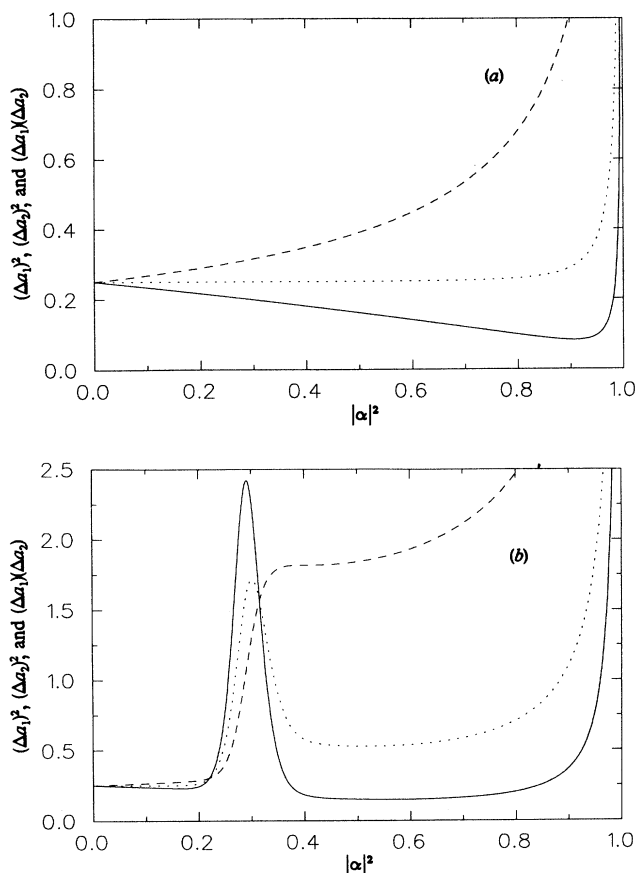


FIG. 4. Squeezing of (a) 1-cotangent states and (b) 3-cotangent states bound between the vacuum and the trapping state $|20\rangle$, as a function of $|\alpha|^2$. The solid line is the variance $(\Delta a_1)^2$, the dashed line is the variance $(\Delta a_2)^2$, and the dotted line is the uncertainty product $(\Delta a_1)(\Delta a_2)$. Here the relative phase between α and β was set at $\pi/2$.

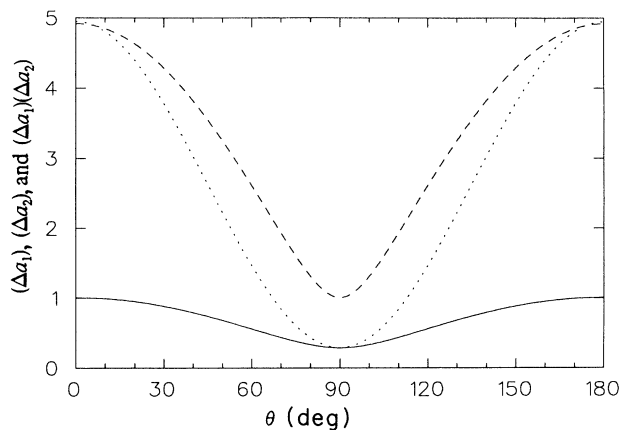


FIG. 5. Standard deviations Δa_1 (solid line) and Δa_2 (dashed line) as well as the uncertainty product $(\Delta a_1)(\Delta a_2)$ (dotted line) plotted against the relative phase between α and β . The field is in the 1-cotangent state with $|\alpha|^2=0.9$ and photon statistics bound between the vacuum and the upper trapping state $|20\rangle$.

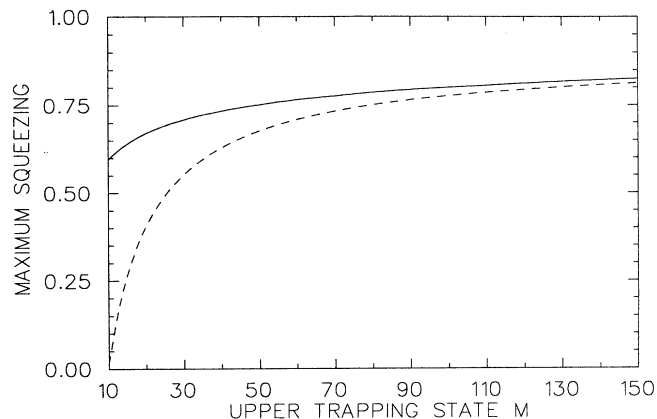


FIG. 6. Squeezing in Δa_1 for the 1-cotangent states (solid line) and 3-cotangent states (dashed line) bound between the vacuum and the trapping state $|M\rangle$ as a function of M . Here $|\alpha|^2$ is chosen at each value of M such that the maximum squeezing is obtained. The relative phase between α and β was set at $\pi/2$. The maximum of the y scale corresponds to 100% squeezing and the minimum to no squeezing.

chosen $|\alpha|^2=0.90$ for 1-cotangent states confined between the vacuum $|0\rangle$ and $|20\rangle$. The cyclical nature of the standard deviations every 180° is easily understood from Eqs. (4.5). The relative phase θ between the two atomic probability amplitudes is translated into the same phase difference between successive probability amplitudes s_n of the cotangent state; see Eq. (2.3). Thus the terms in Eqs. (4.5) that have factors proportional to $s_n s_{n\pm 2}^*$ rotate by 360° when $\theta=180^\circ$. The other two terms with factors $s_n s_{n\pm 1}^*$ get an extra minus sign, but since these terms are squared the minus sign goes away and the resultant expression is identical to the one with $\theta=0^\circ$.

Figure 6 shows the maximum squeezing obtained for 1- and 3-cotangent states (solid and dashed lines, respectively) bound between the vacuum and the trapping state $|M\rangle$ as a function of M . Here the relative phase between α and β is set at $\pi/2$. Instances in which there is an intervening trapping state between $|0\rangle$ and $|M\rangle$ have been excluded.² The amount of squeezing, which initially increases rapidly with increasing M ,²⁰ appears to asymptotically approach 100% as $M \rightarrow \infty$. For $M < 50$, the maximum squeezing occurs in a 1-cotangent state with $|\alpha|^2 \approx 0.90$. However, the optimum value of $|\alpha|^2$ increases as M gets larger. For example, when $M > 200$ the maximum squeezing occurs in cotangent states with $|\alpha|^2 \approx 0.99$.

V. SUMMARY AND CONCLUSIONS

In this paper, we used the Pegg-Barnett phase operator formalism to calculate the phase distribution, phase variance, and number-phase uncertainty product for the 1- and 3-cotangent states. The phase properties illustrate the similarities and differences between these two types of states. In particular, since the 1-cotangent states always have single-peaked photon statistics, their phase never

develops the oscillations that occur in the 3-cotangent states where they acquire the characteristics of "macroscopic superpositions" of states. Both the 1- and 3-cotangent states are nearly minimum number-phase states for a large range of atomic inversions, approximately $0.5 < |\alpha|^2 < 0.9$.

We also calculated the quadrature squeezing of the 1- and 3-cotangent states and found that for increasing $|\alpha|^2$ in the 1-cotangent states the squeezing increases up to a point. For $|\alpha|^2$ close to 1, the cotangent states start to resemble the trapping states $|M\rangle$ and the squeezing disappears. The 3-cotangent states are generally less squeezed than the 1-cotangent states for the same value of $|\alpha|^2$, and the variances $(\Delta a_1)^2$ and $(\Delta a_2)^2$ are quite large in the region of $|\alpha|^2$ where these states resemble a macroscopic superposition. The maximum squeezing of

both types of cotangent states for any $|\alpha|^2$ increases with the upper trapping state M , approaching 100% as $M \rightarrow \infty$. The value of $|\alpha|^2$ of this maximally squeezed cotangent state also increases with M . Reference 12 found that for a given field intensity the squeezing in the Jaynes-Cummings model can become stronger as the detuning between the field mode and the atomic transition frequency increases. In a future paper we will consider the squeezing properties of the steady states of the non-resonant lossless micromaser.

ACKNOWLEDGMENTS

This work is supported by the U. S. Office of Naval Research, Contract No. N00014-88-K-0294, and by the National Science Foundation, Grant No. PHY-8902548.

*Also at: Department of Physics, University of Arizona, Tucson, AZ 85721.

¹J. J. Slosser, P. Meystre, and S. Braunstein, *Phys. Rev. Lett.* **63**, 935 (1989).

²J. J. Slosser and P. Meystre, *Phys. Rev. A* **41**, 3867 (1990).

³J. J. Slosser, P. Meystre, and E. Wright, *Opt. Lett.* **15**, 233 (1990).

⁴L. Susskind and J. Glogower, *Physics* **1**, 49 (1964).

⁵P. Carruthers and M. M. Nieto, *Rev. Mod. Phys.* **40**, 411 (1968).

⁶J. M. Lévy-LeBlond, *Ann. Phys. (N.Y.)* **101**, 319 (1976).

⁷S. M. Barnett and D. T. Pegg, *J. Phys. A* **19**, 3489 (1986).

⁸D. T. Pegg and S. M. Barnett, *Europhys. Lett.* **6**, 483 (1988).

⁹D. T. Pegg and S. M. Barnett, *Phys. Rev. A* **310**, 1665 (1989).

¹⁰S. M. Barnett and D. T. Pegg, *J. Mod. Opt.* **36**, 7 (1989).

¹¹P. Meystre and M. S. Zubairy, *Phys. Lett.* **89A**, 391 (1982).

¹²J. R. Kuklinski and J. L. Madajczyk, *Phys. Rev. A* **37**, 3175

(1988).

¹³P. Filipowicz, J. Javanainen, and P. M. Meystre, *J. Opt. Soc. Am. B* **3**, 906 (1986).

¹⁴P. Meystre and M. Sargent, *Elements of Quantum Optics* (Springer, New York, 1990).

¹⁵R. Loudon, *The Quantum Theory of Light*, 1st ed. (Oxford University Press, Oxford, England, 1973).

¹⁶For a discussion of this point of view in squeezing, see W. Schleich and J. A. Wheeler, *Nature* **326**, 574 (1987).

¹⁷P. Meystre, J. J. Slosser, and M. Wilkens, *Opt. Commun.* **79**, 300 (1990).

¹⁸J. H. Shapiro, S. R. Shepard, and N. C. Wong, in *Coherence and Quantum Optics VI*, edited by J. H. Eberly, L. Mandel, and E. Wolf (Plenum, New York, 1989).

¹⁹S. Qamar, K. Zaheer, and M. S. Zubairy, *Opt. Commun.* **78**, 341 (1990).

²⁰This effect was also noticed in Ref. 19.